Gate-Voltage-Induced Switching of the Spin-Relaxation Rate in a Triple-Quantum-Well Structure

Tomonori Iijima[1] and Hiroshi Akera[2,*]

[1] *Division of Applied Physics, Graduate School of Engineering, Hokkaido University, Sapporo, Hokkaido 060-8628, Japan*

[2] *Division of Applied Physics, Faculty of Engineering, Hokkaido University, Sapporo, Hokkaido 060-8628, Japan*

(Received 30 October 2019; revised manuscript received 27 May 2020; accepted 1 June 2020; published 30 June 2020)

Switching of the Dyakonov-Perel spin relaxation owing to the Rashba spin-orbit interaction (SOI) is theoretically studied in a semiconductor heterostructure with three quantum wells. The action of the present spin-relaxation switching is based on the gate-voltage induced electron transfer from the central well with vanishing Rashba SOI to the left or right well with large Rashba SOI. The spin-relaxation rate is calculated by extending the Dyakonov-Perel theory of the spin relaxation in a single subband to that in more than one subband in order to take into account the contribution from electrons in excited subbands at higher temperatures. It is shown that the on:off ratio of the spin-relaxation rate at room temperature reaches 10^6 by choosing widths and compositions of well and barrier layers so as to reduce electron population in excited subbands, which gives an undesirable spin relaxation. The present spin-relaxation switching is expected to improve the on:off ratio of the current in the spin-lifetime field effect transistor.

DOI: 10.1103/PhysRevApplied.13.064075

I. INTRODUCTION

A number of spin field-effect transistors have been proposed and explored in spintronics [1,2]. Among them the spin FET proposed by Datta and Das [3] has been most extensively studied, which utilizes the precession of electron spin around the effective magnetic field $\mathbf{B}_{\rm eff}$ induced by the Rashba spin-orbit interaction (SOI) [4–7] in a two-dimensional (2D) electron channel. The Rashba SOI is given by $\alpha(\sigma_x k_y - \sigma_y k_x)$, where σ_x and σ_y are the Pauli spin operators, k_x and k_y are wave numbers, and α is the coefficient representing the strength of the Rashba SOI. The realization of this spin FET, however, requires the suppression of the spin relaxation with respect to at least two spin directions in order to maintain the spin precession. Another spin FET, called spin-lifetime FET, has been proposed in several papers [8–11], which uses only the spin polarization along one direction (say, perpendicular to the 2D channel) in contrast to the Datta-Das spin FET and therefore has the advantage that it requires the suppression of the spin relaxation with respect to only one spin direction. In this paper we explore the method to improve the on:off current ratio of the spin-lifetime FET.

The spin-lifetime FET switches the current on and off by switching the spin-relaxation rate between high and low levels. The original method [8–11] for switching the spin-relaxation rate employs the gate-voltage dependence of the Rashba coefficient α in a single symmetric quantum well (QW), confirmed by experiments [12–14], in which $\alpha = a_{\rm so}E_z$ with E_z the electric field perpendicular to the QW produced by the gate voltage and $a_{\rm so}$ the proportionality constant depending on compositions of well and barrier semiconductors. In the Dyakonov-Perel mechanism [15–17] the spin-relaxation rate $1/\tau_s$ is given by $1/\tau_s = b\alpha^2$ (b is the proportionality constant) [18] and, consequently, in a symmetric QW, $1/\tau_s = b(a_{\rm so}E_z)^2$, which leads to the switching of the spin-relaxation rate by changing the gate voltage. The on:off ratio of $1/\tau_s$ could be made arbitrarily large if it is possible to maintain the value of E_z at the infinitesimal in the off state. In a real sample, however, it is difficult to know the exact value of the gate voltage to make E_z vanish because details of the structure, such as the dopant density, should have unknown deviations from the designed value. Then each sample has an inevitable deviation of E_z from 0, which we denote by ΔE_z, when the gate voltage is at the value that gives $E_z = 0$ in the ideal structure. Therefore, the lowest spin-relaxation rate is limited to $b(a_{\rm so}\Delta E_z)^2$.

To overcome such limitation in the lowest spin-relaxation rate of the spin-lifetime FET, in this paper we propose a structure consisting of a wider QW with negligible α and a narrower QW with large $|\alpha|$. By placing a thick barrier between these QWs, electrons are well localized in the wider QW near $E_z = 0$, while they transfer to the narrower QW by applying a large enough E_z, giving the E_z-induced switching of the Rashba coefficient

*akera@eng.hokudai.ac.jp

and consequently the spin-relaxation rate. As a QW with negligible Rashba SOI, we choose a symmetric QW, $B/W/B$, with $W = In_{0.53}Ga_{0.47}As$ (well layer) and $B = Al_xGa_{1-x}As_ySb_{1-y}$ $(x = 0.3)$ (barrier layer) based on our finding [19] that the proportionality constant a_{so} (in $\alpha = a_{so}E_z$) can be made to vanish by tuning the Al fraction of the barrier compound to a value which is close to $x = 0.3$ [20]. Since the Rashba SOI in this QW is suppressed even at nonzero E_z, the lowest spin-relaxation rate and the off current in the spin-lifetime FET can be reduced even when E_z deviates from 0 by ΔE_z. As a QW with large Rashba SOI, we choose an asymmetric QW, $A/W/B$, with two different barrier materials, A and B, where $A = AlAs_ySb_{1-y}$ or $In_{0.52}Al_{0.48}As$, while B and W are the same as the previous QW, $B/W/B$. Since an asymmetric QW exhibits a large $|\alpha|$ even at $E_z = 0$ when the well width is narrow [21], it may contribute to reducing the required gate voltage for switching. Although the simplest structure realizing such switching action is an asymmetric double-QW structure with $A/W/B$ and $B/W/B$, we employ a symmetric triple-QW structure consisting of $A/W/B$, $B/W/B$, and $B/W/A$ as shown in Fig. 1 since it exhibits a simpler E_z dependence of the spin-relaxation rate; in fact, its spin-relaxation rate is 0 at $E_z = 0$ (the center well is made wider than the left and right wells so as to place electrons in the center well at $E_z = 0$). A theoretical estimate for the off value of the spin relaxation rate in the triple-QW

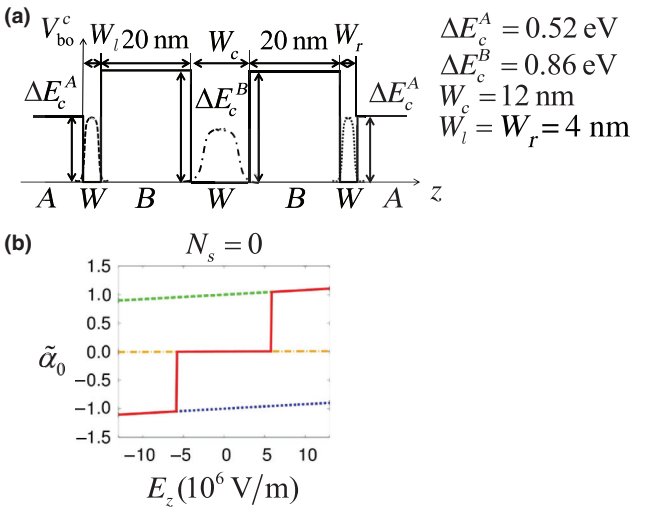

FIG. 1. (a) A triple-QW structure and the potential due to the conduction-band offset $V_{bo}^c(z)$. (b) The dependence on the applied electric field E_z perpendicular to QWs of the normalized Rashba coefficient $\tilde{\alpha}_0$ for an electron in the ground subband at the electron sheet density $N_s = 0$. The dashed, dashed-dotted, and dotted lines represent $\tilde{\alpha}_0$ of $A/W/B$ (left), $B/W/B$ (center), and $B/W/A$ (right) QWs, respectively, where $A = In_{0.52}Al_{0.48}As$, $B = Al_xGa_{1-x}As_ySb_{1-y}$ $(x = 0.3)$, and $W = In_{0.53}Ga_{0.47}As$. In the triple-QW structure $\tilde{\alpha}_0$ (solid line) shows a discontinuous change when the electron makes a transfer between adjacent QWs. Here $\tilde{\alpha}_0$ is normalized so that $\tilde{\alpha}_0 = 1$ for A/W/B at $E_z = 0$.

structure compared to that in a single QW, $A/W/A$, is $(\alpha_{triple}/\alpha_{single})^2 = (a_{so}^{B/W/B}/a_{so}^{A/W/A})^2 \sim 10^{-3}$ for both $A = AlAs_ySb_{1-y}$ and $In_{0.52}Al_{0.48}As$ if we assume that $\alpha_{triple} = \alpha_{B/W/B}$ at small E_z and evaluate α_{triple} and α_{single} at the same value of $E_z = \Delta E_z$.

In evaluating the on:off ratio of the spin-relaxation rate in the proposed triple-QW structure at room temperature, however, we need an extension of the Dyakonov-Perel theory for the spin-relaxation rate [15–17]. At absolute zero electrons occupy only the ground subband of the triple-QW structure when the electron sheet density N_s is small enough and the original Dyakonov-Perel theory for a single band (subband) [15–17] is applicable, which gives the spin-relaxation rate proportional to the square of α_0, the Rashba coefficient in the ground subband $n = 0$. At higher temperatures, however, electrons also occupy excited subbands, which have different Rashba coefficients, α_n $(n \geq 1)$. We therefore need the formula for the spin-relaxation rate $1/T_1$ that is applicable to the case where more than one subband with different Rashba coefficients are occupied [22].

In this paper we extend the Dyakonov-Perel theory for the spin relaxation in a single subband to the multisubband case and derive the formula for the spin-relaxation rate that is applicable to the case with electron occupation in excited subbands. Then we employ the derived formula to evaluate the on:off ratio of the spin-relaxation rate from absolute zero to room temperature in triple-QW structures with different layer widths and compositions. We show that, in a triple-QW structure with a larger energy separation between the ground subband and excited subbands, the on:off ratio of the spin-relaxation rate at room temperature reaches 10^6, which is much larger than the on:off ratio in a single asymmetric QW $(A/W/B)$, which has been proposed in our previous paper [21], and that in a single symmetric QW $(A/W/A)$ used in the original proposal of the spin-lifetime FET [10,11].

This paper is organized as follows. In Sec. II we describe the model and the Hamiltonian of triple-QW structures, based on which we derive the formula for the spin-relaxation rate in the multisubband case in Sec. III. In evaluating the spin-relaxation rate (Sec. IV) we first establish guidelines to achieve a higher on:off ratio of the spin-relaxation rate in Sec. IV A, and then present results of the spin-relaxation rate when we choose $In_{0.52}Al_{0.48}As$ as a barrier material A in Sec. IV B and $AlAs_ySb_{1-y}$ in Sec. IV C. We compare the obtained on:off ratio of the spin-relaxation rate in the triple-QW structure with that in single QWs $A/W/A$ and $A/W/B$ in Sec. IV D. Finally, we present conclusions in Sec. V.

II. MODEL AND HAMILTONIAN

We consider a symmetric triple-QW structure, schematically shown in Fig. 1, which consists of $A/W/B$ (left),

$B/W/B$ (center), and $B/W/A$ (right) QWs, where A, B, and W are semiconductors with the zinc-blende structure. We choose $W = In_{0.53}Ga_{0.47}As$ as the well material, $B = Al_xGa_{1-x}As_ySb_{1-y}$ ($x = 0.3$) as the inner barrier material, and $A = AlAs_ySb_{1-y}$ or $In_{0.52}Al_{0.48}As$ as the outer barrier material (the fraction of As, y, is determined so that the layer is lattice matched to InP). The Rashba coefficient α_0 in the ground subband of the $B/W/B$ QW, which is plotted as a function of E_z, the applied electric field perpendicular to QWs, by a dashed-dotted line in Fig. 1(b), is close to 0 [19], while $|\alpha_0|$ of the $A/W/B$ (dashed line) and $B/W/A$ (dotted line) QWs are large even at $E_z = 0$ [21]. In the triple QW, the electron transfer takes place from the left QW to the center QW and subsequently to the right QW upon changing the force on an electron, $F_z = -eE_z$ ($e > 0$), from negative to positive; consequently, α_0 shows discontinuous changes, shown in Fig. 1(b), leading to the E_z-induced switching of the spin-relaxation rate. In the following we calculate the spin-relaxation rate as a function of E_z in the case where excited subbands are occupied by electrons when the electron sheet density N_s or the temperature is raised.

The Hamiltonian H for a conduction-band electron confined in a triple-QW structure is

$$H = H_{\rm QW} + H_W^{\rm so} + V_{\rm imp}, \tag{1}$$

where $H_{\rm QW}$ describes the motion of an electron in the triple-QW potential, $V_W(z)$, $H_W^{\rm so}$ is the Rashba SOI induced by $V_W(z)$, and $V_{\rm imp}$ is the potential produced by randomly distributed impurities. The QW Hamiltonian $H_{\rm QW}$ is given by

$$H_{\rm QW} = \frac{\hat{\mathbf{p}}^2}{2m} + V_W(z), \tag{2}$$

where $\hat{\mathbf{p}} = (\hat{p}_x, \hat{p}_y, \hat{p}_z) = -i\hbar\nabla = -i\hbar(\nabla_x, \nabla_y, \nabla_z)$ and m is the effective mass of the conduction band. The potential $V_W(z)$ is

$$V_W(z) = V_{\rm bo}^c(z) + V_{\rm es}(z). \tag{3}$$

Here $V_{\rm bo}^c(z)$ is the potential due to conduction-band offsets at interfaces between different layers and is given by

$$V_{\rm bo}^c(z) = \Delta E_c^A h_A(z) + \Delta E_c^B h_B(z), \tag{4}$$

where

$$h_\ell(z) = \begin{cases} 1 & \text{for } z \text{ in barrier } \ell (\ell = A, B), \\ 0 & \text{otherwise,} \end{cases} \tag{5}$$

and conduction band offsets are defined by $\Delta E_c^\ell = E_c^\ell - E_c$ with E_c (E_c^ℓ) the energy of the conduction-band bottom in $In_{0.53}Ga_{0.47}As$ (barrier semiconductor ℓ). The potential $V_{\rm es}(z)$ [the second term of $V_W(z)$] is the electrostatic potential, which is created by the charge density due to electrons within the triple-QW structure and donors outside of the structure and by the applied electric field E_z and is to be calculated self-consistently by the Hartree approximation when $N_s \neq 0$. We apply the periodic boundary conditions in the x and y directions. Then each eigenstate of $H_{\rm QW}$ is labeled by the subband index, $n = 0, 1, 2, \ldots$, the wave vector in the x-y plane, $\mathbf{k} = (k_x, k_y)$, and the z component of the spin, $\sigma = \pm 1$ ($\sigma = \uparrow, \downarrow$). The corresponding eigenvector $|n\mathbf{k}\sigma\rangle$ satisfies

$$H_{\rm QW}|n\mathbf{k}\sigma\rangle = \varepsilon_{n\mathbf{k}\sigma}|n\mathbf{k}\sigma\rangle, \tag{6}$$

where the eigenenergy is

$$\varepsilon_{n\mathbf{k}\sigma} = \varepsilon_n + \hbar^2 k^2/2m, \tag{7}$$

with $k = |\mathbf{k}|$. Here ε_n is the eigenvalue of the Hamiltonian associated with the motion along the z direction,

$$\left[\frac{\hat{p}_z^2}{2m} + V_W(z)\right]|n\rangle = \varepsilon_n|n\rangle, \tag{8}$$

where $|n\rangle$ is the corresponding eigenvector.

The SOI, $H_W^{\rm so}$, is induced by the valence band offsets and the electrostatic potential $V_{\rm es}(z)$ [23–25] and is given by

$$H_W^{\rm so} = a(z)(\sigma_x\hat{k}_y - \sigma_y\hat{k}_x), \tag{9}$$

where $(\hat{k}_x, \hat{k}_y) = (\hat{p}_x, \hat{p}_y)/\hbar$ and

$$a(z) = (\eta_v^A \Delta E_v^A - \eta_s^A \Delta E_s^A)\nabla_z h_A + (\eta_v^B \Delta E_v^B - \eta_s^B \Delta E_s^B)\nabla_z h_B + \eta \nabla_z V_{\rm es}. \tag{10}$$

The expectation value of $H_W^{\rm so}$ is of the form of the Rashba SOI [4–7], i.e.,

$$R_{n\mathbf{k}} \equiv \langle n\mathbf{k}|H_W^{\rm so}|n\mathbf{k}\rangle = \alpha_n(\sigma_x k_y - \sigma_y k_x) \tag{11}$$

with α_n the subband-dependent coefficient defined by

$$\alpha_n = \langle n|a(z)|n\rangle. \tag{12}$$

The factors η_v^ℓ, η_s^ℓ ($\ell = A$, B), and η in Eq. (10) are given by

$$\eta_v^\ell = \frac{P^2}{3}\frac{1}{E_g(E_g - \Delta E_v^\ell)}, \tag{13}$$

$$\eta_s^\ell = \frac{P^2}{3}\frac{1}{E_g^s(E_g^s - \Delta E_s^\ell)}, \tag{14}$$

$$\eta = \frac{P^2}{3}\left[\frac{1}{(E_g)^2} - \frac{1}{(E_g^s)^2}\right]. \tag{15}$$

Here band gaps are defined by $E_g = E_c - E_v$ and $E_g^s = E_c - E_s$, while valence-band offsets are given by

$\Delta E_v^\ell = E_v^\ell - E_v$ and $\Delta E_s^\ell = E_s^\ell - E_s$ with E_v (E_v^ℓ) the energy of the valence-band top and E_s (E_s^ℓ) that of the split-off-band top in the well semiconductor W (barrier semiconductor ℓ). The Kane matrix element [26] P is defined by

$$P = -i\frac{\hbar}{m_0}\langle S|\hat{p}_x|X\rangle, \tag{16}$$

where m_0 is the electron rest mass, while $|S\rangle$ and $|X\rangle$ are the s-type wave function at the conduction-band bottom and the p-type wave function at the valence-band top, respectively.

The impurity potential $V_{\rm imp}(\mathbf{r})$ with $\mathbf{r} = (x, y, z)$ is the potential originating from impurities that are distributed uniformly and randomly in the triple-QW structure. We take the reference point of $V_{\rm imp}(\mathbf{r})$ so that $\int V_{\rm imp}(\mathbf{r})dxdy = 0$. Therefore, its matrix elements diagonal in $\mathbf{k}$ are 0:

$$\langle n'\mathbf{k}\sigma|V_{\rm imp}|n\mathbf{k}\sigma\rangle = 0. \tag{17}$$

Furthermore, we assume that $V_{\rm imp}(\mathbf{r})$ is written as the summation of potentials due to each impurity:

$$V_{\rm imp}(\mathbf{r}) = \sum_i u(\mathbf{r} - \mathbf{r}_i) \tag{18}$$

with $\mathbf{r}_i$ the position vector of the ith impurity.

III. FORMULA FOR THE SPIN-RELAXATION RATE

In this paper we consider the Dyakonov-Perel spin relaxation in a (110)-oriented QW structure for the spin polarization in the [110] direction (z direction) (denoted by S_z) assuming that $S_x = S_y = 0$ and $S_z \neq 0$. Then the Dyakonov-Perel spin relaxation of S_z is caused by the Rashba SOI alone since the Dresselhaus SOI [27] produces the effective magnetic field along z in a (110) QW [17,19,28,29] (see note [30] with regard to off-diagonal components of the spin relaxation rate tensor [31]). The spin-relaxation time τ_s or the spin-relaxation rate τ_s^{-1} for S_z is obtained from

$$\frac{dS_z}{dt} = -\frac{S_z}{\tau_s}, \tag{19}$$

in which S_z is defined by the sum of $s_z = (\hbar/2)\sigma_z$ of each electron and is given by

$$S_z = {\rm tr}(\rho s_z), \tag{20}$$

using the density operator ρ for one-electron states [32]. Here tr$(\cdot)$ is the trace operation with respect to one-electron states. The time derivative dS_z/dt is evaluated by the equation of motion for ρ [32]:

$$i\hbar\frac{d\rho}{dt} = [H, \rho]. \tag{21}$$

Now we calculate S_z and dS_z/dt by choosing the following unperturbed Hamiltonian H_0 and the perturbation $\mathcal{V}$:

$$H = H_0 + \mathcal{V}, \qquad H_0 = H_{\rm QW} + H_W^{\rm so}, \qquad \mathcal{V} = V_{\rm imp}. \tag{22}$$

Using the eigenvectors of $H_{\rm QW}$, $|n\mathbf{k}\sigma\rangle$, as basis vectors, S_z is expressed as

$$S_z = \frac{\hbar}{2}\sum_{n\mathbf{k}\sigma}\langle n\mathbf{k}\sigma|\rho\sigma_z|n\mathbf{k}\sigma\rangle = \frac{\hbar}{2}\sum_{n\mathbf{k}\sigma}\sigma\langle\sigma|f_{n\mathbf{k}}|\sigma\rangle, \tag{23}$$

in which we have introduced an operator in the spin space:

$$f_{n\mathbf{k}} = \langle n\mathbf{k}|\rho|n\mathbf{k}\rangle. \tag{24}$$

In order to obtain dS_z/dt, we derive the equation of motion for $f_{n\mathbf{k}}$. Here we employ the interaction representation such that

$$\rho_I(t) = U^\dagger(t)\rho(t)\,U(t), \qquad \mathcal{V}_I(t) = U^\dagger(t)\mathcal{V}(t)\,U(t), \tag{25}$$

where

$$U(t) = \exp\left(\frac{1}{i\hbar}H_0 t\right). \tag{26}$$

Then we obtain, from Eq. (21),

$$\frac{d\rho_I}{dt} = \frac{1}{i\hbar}[\mathcal{V}_I, \rho_I]. \tag{27}$$

By integrating both sides of this equation from t_0 to t, we have

$$\rho_I(t) = \rho_I(t_0) + \int_{t_0}^{t} dt' \frac{1}{i\hbar}[\mathcal{V}_I(t'), \rho_I(t')]. \tag{28}$$

Substituting this into Eq. (27), we have, up to the second order of $\mathcal{V}$,

$$\frac{d\rho_I}{dt} = \frac{1}{i\hbar}[\mathcal{V}_I(t), \rho_I(t_0)] - \frac{1}{\hbar^2}\int_{t_0}^{t} dt'\{\mathcal{V}_I(t), [\mathcal{V}_I(t'), \rho_I(t)]\}. \tag{29}$$

Writing $\rho_I(t)$ on the left-hand side of the equation in terms of $\rho(t)$, we obtain

$$\frac{d\rho}{dt} = \frac{1}{i\hbar}[H_0, \rho] + \frac{1}{i\hbar}U(t)[\mathcal{V}_I(t), \rho_I(t_0)]U^\dagger(t) + J(t) \tag{30}$$

with

$$J(t) = -\frac{1}{\hbar^2}\int_{t_0}^{t} dt' U(t)\{\mathcal{V}_I(t), [\mathcal{V}_I(t'), \rho_I(t)]\}U^{\dagger}(t). \quad (31)$$

To obtain the equation of motion for $f_{n\mathbf{k}}$, we evaluate diagonal matrix elements $\langle n\mathbf{k}|\cdots|n\mathbf{k}\rangle$ of each term in Eq. (30). In calculating $\langle n\mathbf{k}|[H_W^{\rm so}, \rho]|n\mathbf{k}\rangle$ we employ the approximation that

$$\langle n'\mathbf{k}|\rho|n\mathbf{k}\rangle = 0 \quad (n \neq n'), \quad (32)$$

which is valid when the energy difference $\varepsilon_{n'\mathbf{k},-\sigma} - \varepsilon_{n\mathbf{k}\sigma}$ is large compared to the absolute value of $\langle n'\mathbf{k}, -\sigma|H_W^{\rm so}|n\mathbf{k}\sigma\rangle$. In evaluating terms with $\mathcal{V}_I$ in Eq. (30), we take the average with respect to the x and y coordinates of each impurity and use Eq. (17). Then we obtain

$$\frac{df_{n\mathbf{k}}}{dt} = \frac{1}{i\hbar}[R_{n\mathbf{k}}, f_{n\mathbf{k}}] + J_{n\mathbf{k}} \quad (33)$$

with $J_{n\mathbf{k}} = \langle n\mathbf{k}|J(t)|n\mathbf{k}\rangle$. In evaluating $J_{n\mathbf{k}}$ we neglect $H_W^{\rm so}$ according to the Dyakonov-Perel theory [16] and take the limit of $t_0 \to -\infty$. Then $J_{n\mathbf{k}}$ reduces to

$$J_{n\mathbf{k}} = \sum_{n'\mathbf{k}'}[-W_{n'\mathbf{k}',n\mathbf{k}} f_{n\mathbf{k}}(t) + W_{n\mathbf{k},n'\mathbf{k}'} f_{n'\mathbf{k}'}(t)], \quad (34)$$

where $W_{n'\mathbf{k}',n\mathbf{k}}$ is the spin-independent transition rate from $n\mathbf{k}$ to $n'\mathbf{k}'$ given by

$$W_{n'\mathbf{k}',n\mathbf{k}} = \frac{2\pi}{\hbar}|\langle n'\mathbf{k}'\,|V_{\rm imp}|\,n\mathbf{k}\rangle|^2 \delta(\varepsilon_{n'\mathbf{k}'} - \varepsilon_{n\mathbf{k}}), \quad (35)$$

which is proportional to the impurity volume density since it reduces to the summation of the transition rate at each impurity after the average with respect to the x and y coordinates of each impurity is taken.

Since $df_{n\mathbf{k}}/dt$, which determines dS_z/dt, is given in Eq. (33) by $f_{n\mathbf{k}}$, we solve Eq. (33) for $f_{n\mathbf{k}}$ up to the first order of $R_{n\mathbf{k}}$. We express $H_W^{\rm so}$ [Eq. (9)] and $R_{n\mathbf{k}} = \langle n\mathbf{k}|H_{\rm W}^{\rm so}|n\mathbf{k}\rangle$ [Eq. (11)] by the effective magnetic field operator $\hat{\mathbf{\Omega}} = (\hat{\Omega}_x, \hat{\Omega}_y, 0)$ [16] and its expectation value $\mathbf{\Omega}_n(\mathbf{k}) \equiv \langle n\mathbf{k}|\hat{\mathbf{\Omega}}|n\mathbf{k}\rangle$, respectively:

$$H_W^{\rm so} = \frac{\hbar}{2}\hat{\mathbf{\Omega}}\cdot\boldsymbol{\sigma}, \qquad R_{n\mathbf{k}} = \frac{\hbar}{2}\mathbf{\Omega}_n(\mathbf{k})\cdot\boldsymbol{\sigma}. \quad (36)$$

Then the strength of the effective magnetic field is given by

$$\Omega_n(k) = |\mathbf{\Omega}_n(\mathbf{k})|, \quad (37)$$

which does not depend on the direction of $\mathbf{k}$. The two terms on the right-hand side of Eq. (33) show that the relative strength of the SOI is given by a dimensionless constant $\Omega\tau$ with Ω the typical value of Ω_n for various subbands and τ the mean free time between successive impurity scatterings. According to Dyakonov and Perel [16], we expand $f_{n\mathbf{k}}$ with respect to $\Omega\tau$ and retain terms of the zeroth order and first order in $\Omega\tau$:

$$f_{n\mathbf{k}} = f_{n\mathbf{k}}^{(0)} + f_{n\mathbf{k}}^{(1)}. \quad (38)$$

Because $df_{n\mathbf{k}}/dt$ is proportional to $1/\tau_s \sim \Omega^2\tau$, as we will see later from the obtained $f_{n\mathbf{k}}^{(0)}$ and $f_{n\mathbf{k}}^{(1)}$, Eq. (33) becomes, in the zeroth order with respect to $\Omega\tau$, $\sum_{n'\mathbf{k}'} W_{n'\mathbf{k}',n\mathbf{k}}(-f_{n\mathbf{k}}^{(0)} + f_{n'\mathbf{k}'}^{(0)}) = 0$, which is satisfied if $f_{n\mathbf{k}}^{(0)}$ is a function of $\varepsilon_{n\mathbf{k}}$. Here we choose $f_{n\mathbf{k}}^{(0)}$ to be a thermal-equilibrium distribution with nonzero S_z:

$$f_{n\mathbf{k}}^{(0)} = \tfrac{1}{2}I[f_{\uparrow}(\varepsilon_{n\mathbf{k}}) + f_{\downarrow}(\varepsilon_{n\mathbf{k}})] + \tfrac{1}{2}\sigma_z f_z(\varepsilon_{n\mathbf{k}}). \quad (39)$$

Here I is the unit matrix and $f_z(\varepsilon_{n\mathbf{k}})$ is the difference in distribution between spin-up and spin-down electrons, i.e.,

$$f_z(\varepsilon_{n\mathbf{k}}) = f_{\uparrow}(\varepsilon_{n\mathbf{k}}) - f_{\downarrow}(\varepsilon_{n\mathbf{k}}), \quad (40)$$

with the spin-dependent Fermi-Dirac distribution function,

$$f_{\sigma}(\varepsilon) = \left[1 + \exp\left(\frac{\varepsilon - \mu_{\sigma}}{k_B T}\right)\right]^{-1}. \quad (41)$$

The spin-dependent chemical potential, μ_{σ}, gives rise to the spin polarization S_z:

$$S_z = \frac{\hbar}{2}\sum_{n\mathbf{k}\sigma}\sigma\langle\sigma|f_{n\mathbf{k}}^{(0)}|\sigma\rangle = \frac{\hbar}{2}\sum_{n\mathbf{k}} f_z(\varepsilon_{n\mathbf{k}}). \quad (42)$$

In the first order with respect to $\Omega\tau$, Eq. (33) becomes

$$\frac{1}{i\hbar}[R_{n\mathbf{k}}, f_{n\mathbf{k}}^{(0)}] + \sum_{n'\mathbf{k}'} W_{n'\mathbf{k}',n\mathbf{k}}(-f_{n\mathbf{k}}^{(1)} + f_{n'\mathbf{k}'}^{(1)}) = 0, \quad (43)$$

which is the equation for $f_{n\mathbf{k}}^{(1)}$. Since we obtain $[R_{n\mathbf{k}}, f_{n\mathbf{k}}^{(0)}] = -i\alpha_n f_z(\varepsilon_{n\mathbf{k}})(\sigma_x k_x + \sigma_y k_y)$ using Eq. (11), Eq. (43) has a solution of the form

$$f_{n\mathbf{k}}^{(1)} = \frac{\tau_n}{i\hbar}[R_{n\mathbf{k}}, f_{n\mathbf{k}}^{(0)}] \quad (44)$$

with a relaxation time $\tau_n(k)$ independent of the direction of $\mathbf{k}$ when $W_{n'\mathbf{k}',n\mathbf{k}}$ is an even function of θ, the angle of $\mathbf{k}'$ relative to $\mathbf{k}$. The relaxation time $\tau_n(\varepsilon)$ for each subband is

determined by

$$P_n(\varepsilon)\tau_n(\varepsilon) - \sum_{n'} Q_{nn'}(\varepsilon)\tau_{n'}(\varepsilon)\frac{\alpha_{n'}k_{n'}(\varepsilon)}{\alpha_n k_n(\varepsilon)} = 1 \tag{45}$$

with

$$P_n(\varepsilon) = \sum_{n'\mathbf{k}'} W_{n'\mathbf{k}',n\mathbf{k}}, \qquad Q_{nn'}(\varepsilon) = \sum_{\mathbf{k}'} W_{n'\mathbf{k}',n\mathbf{k}}\cos\theta, \tag{46}$$

where $k_n(\varepsilon)$ is the value of $|\mathbf{k}|$ satisfying $\varepsilon_{n\mathbf{k}} = \varepsilon$.

The time derivative of S_z is calculated from the solution of $f_{n\mathbf{k}}$ by

$$\frac{dS_z}{dt} = \frac{\hbar}{2}\sum_{n\mathbf{k}\sigma}\sigma\left\langle\sigma\left|\frac{df_{n\mathbf{k}}}{dt}\right|\sigma\right\rangle, \tag{47}$$

with Eq. (33). The collision term in Eq. (33) does not contribute to dS_z/dt because $\sum_{n\mathbf{k}} J_{n\mathbf{k}} = 0$. Since $\sum_{\mathbf{k}}[R_{n\mathbf{k}},f^{(0)}_{n\mathbf{k}}] = 0$ and $[R_{n\mathbf{k}},f^{(1)}_{n\mathbf{k}}] = -2i\hbar^{-1}\tau_n(\varepsilon_{n\mathbf{k}})\alpha_n^2k^2\sigma_z f_z(\varepsilon_{n\mathbf{k}})$, we obtain

$$\frac{dS_z}{dt} = -2\hbar^{-1}\sum_{n\mathbf{k}}\tau_n(\varepsilon_{n\mathbf{k}})\alpha_n^2k^2f_z(\varepsilon_{n\mathbf{k}}). \tag{48}$$

Substituting dS_z/dt derived here and S_z in Eq. (42) into Eq. (19), we obtain the spin-relaxation time τ_s. When $|\mu_\uparrow - \mu_\downarrow| \ll k_BT$, τ_s becomes independent of $\mu_\uparrow - \mu_\downarrow$ and is given by

$$\frac{1}{\tau_s} = \left[\sum_{n=0}^{\infty} f(\varepsilon_n)\right]^{-1}\sum_{n=0}^{\infty}\int_{\varepsilon_n}^{\infty} d\varepsilon\left(-\frac{df}{d\varepsilon}\right)\Omega_n^2(\varepsilon)\tau_n(\varepsilon), \tag{49}$$

where $f(\varepsilon)$ is the Fermi-Dirac distribution function with spin-independent chemical potential $\mu = \mu_\uparrow = \mu_\downarrow$. In our triple-QW structure, Fig. 1 shows that the effective magnetic field strength in the ground subband, $\Omega_0 = (2/\hbar)\alpha_0 k$, is almost 0 in the vicinity of $E_z = 0$ (off region) and therefore the spin relaxation in the off region is caused by electrons in excited subbands through terms of $n \geq 1$ in Eq. (49). Considering such contributions from excited subbands is indispensable in accurately evaluating the on:off ratio of the spin relaxation rate.

IV. CALCULATED RESULTS OF THE SPIN-RELAXATION RATE

A. Guidelines for improving the on:off ratio of the spin-relaxation rate

Our goal in this paper is to propose a quantum well structure which realizes a higher on:off ratio of the spin-relaxation rate in the temperature range from absolute zero to room temperature. For this purpose, we use the E_z-induced electron transfer from a QW with negligible Rashba SOI ($B/W/B$ in the center) at $E_z \sim 0$ to a QW with large Rashba SOI ($A/W/B$ and $B/W/A$ in the left and right, respectively) at large $|E_z|$, as explained in the Introduction, where the well material W is $In_{0.53}Ga_{0.47}As$, one barrier material B is $Al_xGa_{1-x}As_ySb_{1-y}$ ($x = 0.3$) whose composition is adjusted to give $a_{so} \approx 0$, and another barrier material A is $In_{0.52}Al_{0.48}As$ in Sec. IV B and $AlAs_ySb_{1-y}$ in Sec. IV C. To obtain a larger Rashba SOI in $A/W/B$ and $B/W/A$, we choose a narrower well width [21].

At higher temperatures, electrons occupy excited subbands. Electrons in some excited subbands have a large probability density in the left or right well even in the vicinity of $E_z = 0$ and are subject to significant spin relaxation. In order to suppress such undesired spin relaxation in the off region, we need to decrease the electron population in excited subbands by increasing the energy separation between the ground and excited subbands. This can be implemented by increasing the center-well width and decreasing the widths of the left and right wells.

It is also desirable to reduce the magnitude of the electric field, E_z^{trans}, at which the electron transfer occurs from the center to left (or right) well. The required value of E_z^{trans} can be roughly estimated from $eE_z^{trans}\Delta z_{well} = \Delta\varepsilon_{well}$, where Δz_{well} is the distance between the center and left wells and $\Delta\varepsilon_{well}$ is the difference in energy of the lowest bound state between the center and left wells at $E_z = 0$. Thus, we can reduce E_z^{trans} by increasing the width of barrier B.

B. A triple-quantum-well structure with $A = In_{0.52}Al_{0.48}As$

First we adopt $In_{0.52}Al_{0.48}As$ as a barrier material A. In Fig. 2 we present a triple-QW structure designed according to the guidelines in Sec. IV A: the width of the center well is much larger than that of the left and right wells.

In calculating the spin-relaxation rate, we assume that the range of impurity potential is short compared to the

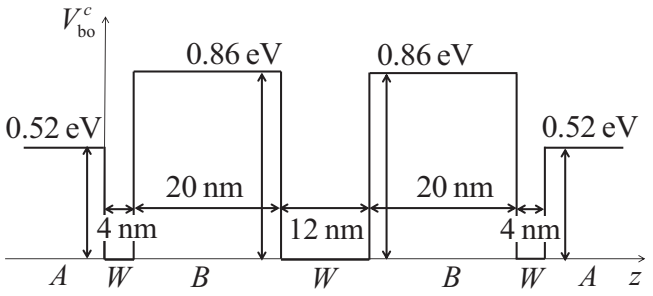

FIG. 2. A triple-QW structure and the potential due to the conduction-band offset $V^c_{bo}(z)$. Barrier materials $A = In_{0.52}Al_{0.48}As$, $B = Al_xGa_{1-x}As_ySb_{1-y}$ ($x = 0.3$), and a well material $W = In_{0.53}Ga_{0.47}As$.

Fermi wavelength, so that

$$u(\mathbf{r}) = u_0\delta(\mathbf{r}). \tag{50}$$

Then we choose, as units of the momentum-relaxation time and the spin-relaxation time, τ_{p0} and τ_{s0}, given by

$$\frac{1}{\tau_{p0}} = n_{\rm imp}u_0^2\frac{m}{\hbar^3 a_B^*}, \tag{51}$$

$$\frac{1}{\tau_{s0}} = 10^6\frac{\eta^2(\mathrm{Ry}^*)^2}{\hbar^2(a_B^*)^4}\tau_{p0} = 10^6\frac{\eta^2\hbar(\mathrm{Ry}^*)^2}{n_{\rm imp}u_0^2 m(a_B^*)^3}, \tag{52}$$

respectively with $n_{\rm imp}$ the impurity volume density. Here $a_B^* = \hbar^2\epsilon/(me^2)$ and $\mathrm{Ry}^* = \hbar^2(a_B^*)^{-2}/(2m)$, which we use as units of length and energy, respectively, with ϵ the static dielectric constant. Their values are $a_B^* = 17.1$ nm and $\mathrm{Ry}^* = 3.04$ meV in $In_{0.53}Ga_{0.47}As$.

In Fig. 3 we present the spin-relaxation rate $1/\tau_s$ of the triple-QW structure shown in Fig. 2 at $T = 0$ K as a function of E_z for three values of N_s, the electron sheet density: $N_s/(10^{11}\ \mathrm{cm}^{-2}) = 4$, 5, and 6. When N_s is nonzero, the electron transfer from the center to the left or right well and the resulting increase of the spin-relaxation rate from "off" to "on" values take place in an E_z range proportional to N_s, followed by a discontinuous increase at a value of E_z, which we denote by $E_z^{\rm on}$. We assign the larger value of $1/\tau_s$ at $E_z = E_z^{\rm on}$ to be the "on" value of the spin-relaxation rate and choose $1/\tau_s$ at $E_z = E_z^{\rm off} = 0.1E_z^{\rm on}$ as the "off" value of the spin-relaxation rate. Then the on:off ratio of the spin-relaxation rate becomes 10^6, which weakly depends on N_s.

The "off" spin-relaxation rate at $T = 0$ K strongly depends on the deviation of the Al fraction x in barrier material B ($Al_xGa_{1-x}As_ySb_{1-y}$) from the value x_0 where the Rashba SOI exactly vanishes in the $B/W/B$ single QW: it is approximately $x_0 \approx 0.28511$. In Fig. 4 we present the

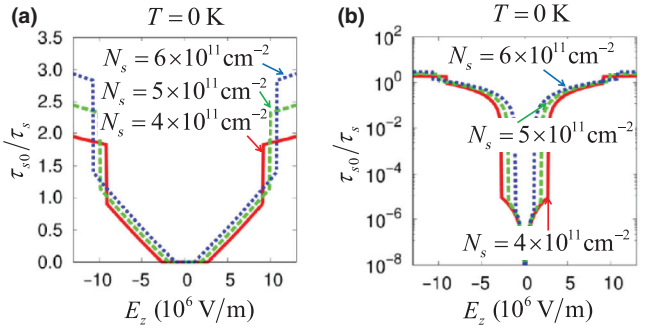

FIG. 3. Electron sheet density N_s dependence of the spin-relaxation rate $1/\tau_s$ at $T = 0$ K as a function of the perpendicular electric field E_z. Barrier material A is $In_{0.52}Al_{0.48}As$. Plotted in (a) linear scale and (b) semilogarithmic scale.

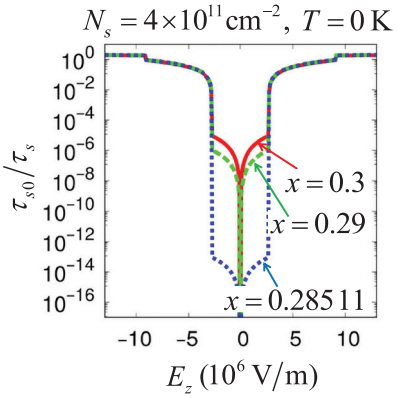

FIG. 4. Decreased spin-relaxation rate $1/\tau_s$ (plotted in semilogarithmic scale) as the Al fraction x in barrier material B ($Al_xGa_{1-x}As_ySb_{1-y}$) approaches the exact value, $x_0(\approx 0.285\,11)$, which gives the vanishing Rashba SOI in the $B/W/B$ single QW. Barrier material A is $In_{0.52}Al_{0.48}As$.

spin-relaxation rate at $x = 0.285\,11$, 0.29, and 0.3 when $N_s = 4\times10^{11}\ \mathrm{cm}^{-2}$ and $T = 0$ K.

In Fig. 5 we present the temperature dependence of the spin-relaxation rate at $N_s = 4\times10^{11}\ \mathrm{cm}^{-2}$. As the temperature is elevated to room temperature, the on:off ratio of the spin-relaxation rate decreases to 10^1 owing to contributions of excited subbands to the "off" spin-relaxation rate. Although in Fig. 5 we have presented the spin-relaxation rate at $x = 0.3$, it shows little difference between $x = 0.3$ and $x = x_0$ at $T \geq 100$ K.

C. A triple-quantum-well structure with $A = AlAs_ySb_{1-y}$

Next we adopt $AlAs_ySb_{1-y}$ as a barrier material A. Since $AlAs_ySb_{1-y}$ gives a larger conduction-band offset at the W/A interface compared to $In_{0.52}Al_{0.48}As$, the $B/W/A$ QW in this case can support a higher-energy bound state at a

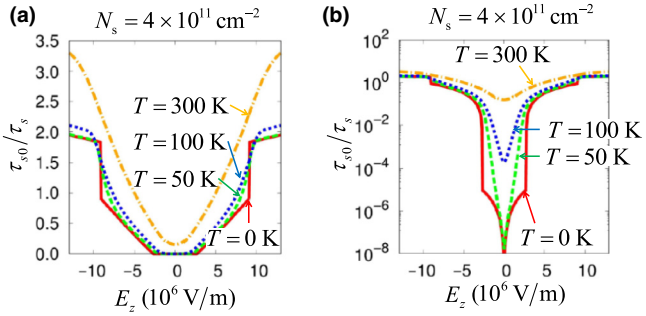

FIG. 5. Temperature dependence of the spin-relaxation rate $1/\tau_s$ as a function of the perpendicular electric field E_z. Temperature values are T[K] = 0, 50, 100, and 300. Barrier material A is $In_{0.52}Al_{0.48}As$. Plotted in (a) linear scale and (b) semilogarithmic scale.

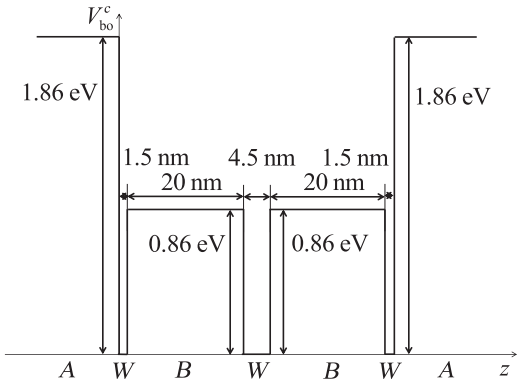

FIG. 6. A triple-QW structure and the potential due to the conduction-band offset $V^c_{bo}(z)$. Barrier materials $A = AlAs_ySb_{1-y}$, $B = Al_xGa_{1-x}As_ySb_{1-y}$ $(x = 0.3)$, and a well material $W = In_{0.53}Ga_{0.47}As$.

narrower well width, which allows the design of a triple-QW structure with reduced electron population in excited subbands in the low E_z region. In Fig. 6 we present such a triple-QW structure.

In Fig. 7 we present the temperature dependence of the spin-relaxation rate of the triple-QW structure shown in Fig. 6 at $N_s = 4 \times 10^{11}$ cm^{-2}. Even at room temperature, the on:off ratio of the spin-relaxation rate attains a high value of 10^6 owing to reduced contributions of excited subbands to the "off" spin-relaxation rate.

D. Comparison with single quantum wells

The room-temperature on:off ratio of the spin-relaxation rate, 10^6, attained in the triple-QW structure (see Fig. 6) is orders of magnitude larger than those in single QWs, as shown in Fig. 8, in which we present the comparison of the room-temperature spin-relaxation rate at $N_s = 4 \times 10^{11}$ cm^{-2} in the triple QW with those in a symmetric QW, $A/W/A$, and an asymmetric QW, $A/W/B$: materials A, B, and W are the same as those in the triple QW (see Fig. 6). We find that the "off" spin-relaxation rate is remarkably reduced in the triple QW compared to $A/W/A$, as expected and explained in the Introduction. In addition, the "on" spin-relaxation rate is significantly enhanced in the triple QW compared to both $A/W/A$ and $A/W/B$ owing to the large Rashba SOI in a narrow asymmetric QW (left and right wells in the triple QW).

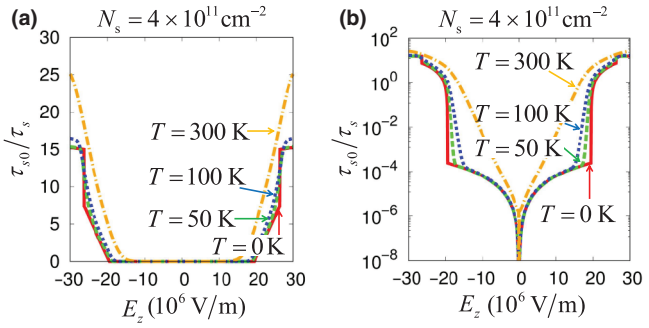

FIG. 7. Temperature dependence of the spin-relaxation rate $1/\tau_s$ as a function of the perpendicular electric field E_z. Temperature values are T[K] = 0, 50, 100, and 300. Barrier material A is $AlAs_ySb_{1-y}$. Plotted in (a) linear scale and (b) semilogarithmic scale.

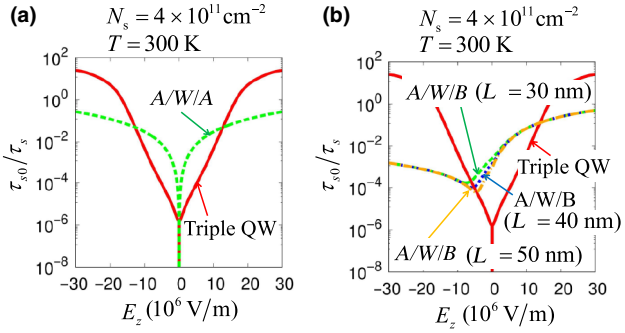

FIG. 8. Room-temperature spin-relaxation rate $1/\tau_s$ as a function of the perpendicular electric field E_z (plotted in semilogarithmic scale) in the triple QW with $AlAs_ySb_{1-y}$ in outer barriers (Fig. 6) is compared to that in single QWs, (a) $A/W/A$ and (b) $A/W/B$, where materials A, B, and W are the same as those in the triple QW. The well width L of $A/W/A$ is 4.5 nm (the on:off ratio of $1/\tau_s$ shows little difference between $L = 4.5$ nm and $L = 50$ nm). The spin-relaxation rate $1/\tau_s$ of $A/W/B$ is presented for three values of the well width, $L = 30, 40$, and 50 nm.

V. CONCLUSIONS

We propose the switching of the spin-relaxation rate by the gate-voltage induced electron transfer between one QW with negligible Rashba SOI and another with large Rashba SOI. We design a triple-QW structure so as to achieve a high on:off ratio of the spin-relaxation rate in the present switching action and realize a room-temperature on:off ratio of 10^6 by reducing the electron population in excited subbands. This value of on:off ratio is orders of magnitude larger than those in single QWs. In calculating the spin-relaxation rate we extend the Dyakonov-Perel theory [15–17] in order to take into account the contribution from excited subbands.

Electron transfer between two QWs and the resulting change in electronic properties have been studied for a long time [33–37]. In this paper we employ the interwell electron transfer for switching the Rashba SOI and the spin-relaxation rate. Here we propose two more examples in spintronics of the switching by the interwell electron transfer.

(1) Switching of the direction and the magnitude of the current-induced spin polarization (called the Edelstein

effect) [38,39] by the electron transfer between two QWs with different Rashba coefficients.

(2) Switching of the precession direction and frequency of an electron spin in a magnetic field by the electron transfer between two QWs with different g factors. A positive (negative) g factor in a QW can be realized by using direct-band-gap semiconductors InP [40–42] ((In,Ga)As [42–45]) as a well material.

One of important performance characteristics of the interwell electron transfer is the time required for an electron to transfer between wells. We estimate the frequency of the interwell transfer, $\omega_{\rm tr}$, from the energy separation, $E_{\rm b-ab}$, between the bonding and antibonding states formed of bound states in neighboring wells by the formula $\hbar\omega_{\rm tr} = E_{\rm b-ab}$. The estimated value of $\omega_{\rm tr}$ in the triple-QW structure in Fig. 6 is of the order of 0.1 GHz.

In this paper we consider only the impurity scattering in evaluating the momentum relaxation for the Dyakonov-Perel spin relaxation. It is well known that at room temperature the phonon scattering makes a significant contribution to the momentum relaxation. In fact, a previous theoretical study [46] calculated the Dyakonov-Perel spin-relaxation rate with the phonon scattering taken into account as a source of the momentum relaxation. However, we expect that the present estimate for the on:off ratio of the spin-relaxation rate will be little affected by considering the momentum relaxation due to the phonon scattering in addition to that due to the impurity scattering since it is mainly determined by orders of magnitude differences in the Rashba SOI strength and in the electron population between the central and left (and right) QWs.

ACKNOWLEDGMENTS

This work was supported by Grant-in-Aid for Scientific Research (C) under Grant No. JP17K05484 from the Japan Society for the Promotion of Science (JSPS).

[1] I. Žutić, J. Fabian, and S. D. Sarma, Spintronics: Fundamentals and applications, Rev. Mod. Phys. **76**, 323 (2004).
[2] D. D. Awschalom and M. E. Flatté, Challenges for semiconductor spintronics, Nat. Phys. **3**, 153 (2007).
[3] S. Datta and B. Das, Electronic analog of the electro-optic modulator, Appl. Phys. Lett. **56**, 665 (1990).
[4] E. I. Rashba, Properties of semiconductors with an extremum loop. 1. Cyclotron and combinational resonance in a magnetic field perpendicular to the plane of the loop, Sov. Phys. Solid State **2**, 1109 (1960).
[5] F. J. Ohkawa and Y. Uemura, Quantized surface states of a narrow-gap semiconductor, J. Phys. Soc. Jpn. **37**, 1325 (1974).
[6] Y. A. Bychkov and E. I. Rashba, Oscillatory effects and the magnetic susceptibility of carriers in inversion layers, J. Phys. C **17**, 6039 (1984).
[7] Y. A. Bychkov and E. I. Rashba, Properties of a 2D electron gas with lifted spectral degeneracy, JETP Lett. **39**, 78 (1984).
[8] J. Schliemann, J. C. Egues, and D. Loss, Nonballistic Spin-Field-Effect Transistor, Phys. Rev. Lett. **90**, 146801 (2003).
[9] X. Cartoixà, D. Z.-Y. Ting, and Y.-C. Chang, A resonant spin lifetime transistor, Appl. Phys. Lett. **83**, 1462 (2003).
[10] K. C. Hall, W. H. Lau, K. Gündoğdu, M. E. Flatté, and T. F. Boggess, Nonmagnetic semiconductor spin transistor, Appl. Phys. Lett. **83**, 2937 (2003).
[11] K. C. Hall and M. E. Flatté, Performance of a spin-based insulated gate field effect transistor, Appl. Phys. Lett. **88**, 162503 (2006).
[12] J. Nitta, T. Akazaki, H. Takayanagi, and T. Enoki, Gate Control of Spin-Orbit Interaction in an Inverted $In_{0.53}Ga_{0.47}As/In_{0.52}Al_{0.48}As$ Heterostructure, Phys. Rev. Lett. **78**, 1335 (1997).
[13] G. Engels, J. Lange, T. Schäpers, and H. Lüth, Experimental and theoretical approach to spin splitting in modulation-doped $In_xGa_{1-x}As/InP$ quantum wells for $B \to 0$, Phys. Rev. B **55**, R1958 (1997).
[14] T. Koga, J. Nitta, T. Akazaki, and H. Takayanagi, Rashba Spin-Orbit Coupling Probed by the Weak Antilocalization Analysis in InAlAs/InGaAs/InAlAs Quantum Wells as a Function of Quantum Well Asymmetry, Phys. Rev. Lett. **89**, 046801 (2002).
[15] M. I. Dyakonov and V. I. Perel, Spin orientation of electrons associated with the interband absorption of light in semiconductors, Sov. Phys. JETP **33**, 1053 (1971).
[16] M. I. Dyakonov and V. I. Perel, Spin relaxation of conduction electrons in noncentrosymmetric semiconductors, Sov. Phys. Solid State **13**, 3023 (1972).
[17] M. I. Dyakonov and V. Y. Kachorovskii, Spin relaxation of two-dimensional electrons in noncentrosymmetric semiconductors, Sov. Phys. Semicond. **20**, 110 (1986).
[18] In this paper we consider the Dyakonov-Perel spin relaxation in QW structures parallel to the (110) plane for the spin polarization perpendicular to the (110) plane. In this case the Dresselhaus SOI [27] gives no spin relaxation since it produces the effective magnetic field perpendicular to the (110) plane [17,19,28,29].
[19] H. Akera, H. Suzuura, and Y. Egami, Spin relaxation in a quantum well by phonon scatterings, Phys. Rev. B **92**, 205311 (2015).
[20] The vanishing of the Rashba SOI in quantum wells can also be realized [47] by introducing a potential produced by the interface dipole [48,49].
[21] H. Akera, H. Suzuura, and Y. Egami, Gate-voltage-induced switching of the Rashba spin-orbit interaction in a composition-adjusted quantum well, Phys. Rev. B **95**, 045301 (2017).
[22] With respect to the spin-dephasing time T_2 Weng and Wu [50] have theoretically studied the role of excited subbands in n-type GaAs QWs. Kaneko, Koshino, and Ando [51] have performed a numerical study of the spin relaxation in a quantum wire with several subbands occupied by electrons.
[23] R. Lassnig, $\mathbf{k}\cdot\mathbf{p}$ theory, effective-mass approach, and spin splitting for two-dimensional electrons in GaAs-GaAlAs heterostructures, Phys. Rev. B **31**, 8076 (1985).

[24] E. Bernardes, J. Schliemann, M. Lee, J. C. Egues, and D. Loss, Spin-Orbit Interaction in Symmetric Wells with two Subbands, Phys. Rev. Lett. **99**, 076603 (2007).

[25] R. S. Calsaverini, E. Bernardes, J. C. Egues, and D. Loss, Intersubband-induced spin-orbit interaction in quantum wells, Phys. Rev. B **78**, 155313 (2008).

[26] E. O. Kane, Band structure of indium antimonide, J. Phys. Chem. Solids **1**, 249 (1957).

[27] G. Dresselhaus, Spin-orbit coupling effects in zinc blende structures, Phys. Rev. **100**, 580 (1955).

[28] R. Winkler, Spin orientation and spin precession in inversion-asymmetric quasi-two-dimensional electron systems, Phys. Rev. B **69**, 045317 (2004).

[29] X. Cartoixà, L.-W. Wang, D.-Y. Ting, and Y.-C. Chang, Higher-order contributions to Rashba and Dresselhaus effects, Phys. Rev. B **73**, 205341 (2006).

[30] In the presence of both Rashba and Dresselhaus SOIs in a (110)-oriented QW structure, *yz* and *zy* components of the spin relaxation rate tensor appear and the principal axis of the tensor deviates from the *z* axis [31]. However, the deviation of the principal axis is very small in the off region of the spin relaxation where the Rashba SOI is much smaller than the Dresselhaus SOI and in the on region of the spin relaxation where the Rashba SOI is much larger than the Dresselhaus SOI.

[31] X. Cartoixà, D. Z.-Y. Ting, and Y.-C. Chang, Suppression of the D'yakonov-Perel' spin-relaxation mechanism for all spin components in [111] zincblende quantum wells, Phys. Rev. B **71**, 045313 (2005).

[32] W. Kohn and J. M. Luttinger, Quantum theory of electrical transport phenomena, Phys. Rev. **108**, 590 (1957).

[33] K. Hess, H. Morkoç, H. Shichijo, and B. G. Streetman, Negative differential resistance through real-space electron transfer, Appl. Phys. Lett. **35**, 469 (1979).

[34] M. Keever, H. Shichijo, K. Hess, S. Banerjee, L. Witkowski, H. Morkoç, and B. G. Streetman, Measurements of hot-electron conduction and real-space transfer in GaAs-$Al_xGa_{1-x}As$ heterojunction layers, Appl. Phys. Lett. **38**, 36 (1981).

[35] N. Sawaki, M. Suzuki, Y. Takagaki, H. Goto, I. Akasaki, H. Kano, Y. Tanaka, and M. Hashimoto, Photoluminescence studies of hot electrons and real space transfer effect in a double quantum well superlattice, Superlattice Microst. **2**, 281 (1986).

[36] N. Sawaki, M. Suzuki, E. Okuno, H. Goto, I. Akasaki, H. Kano, Y. Tanaka, and M. Hashimoto, Real space transfer of two dimensional electrons in double quantum well structures, Solid-State Electron. **31**, 351 (1988).

[37] Z. S. Gribnikov, K. Hess, and G. A. Kosinovsky, Nonlocal and nonlinear transport in semiconductors: Real-space transfer effects, J. Appl. Phys. **77**, 1337 (1995).

[38] V. Edelstein, Spin polarization of conduction electrons induced by electric current in two-dimensional asymmetric electron systems, Solid State Commun. **73**, 233 (1990).

[39] C. L. Yang, H. T. He, L. Ding, L. J. Cui, Y. P. Zeng, J. N. Wang, and W. K. Ge, Spectral Dependence of Spin Photocurrent and Current-Induced Spin Polarization in an InGaAs/InAlAs Two-Dimensional Electron Gas, Phys. Rev. Lett. **96**, 186605 (2006).

[40] C. Weisbuch and C. Hermann, Optical detection of conduction electron spin resonance in InP, Solid State Commun. **16**, 659 (1975).

[41] M. Oestreich, S. Hallstein, A. P. Heberle, K. Eberl, E. Bauser, and W. W. Rühle, Temperature and density dependence of the electron Landé g factor in semiconductors, Phys. Rev. B **53**, 7911 (1996).

[42] H. Kosaka, A. A. Kiselev, F. A. Baron, Ki Wook Kim, and E. Yablonovitch, Electron g factor engineering in III-V semiconductors for quantum communications, Electron. Lett. **37**, 464 (2001).

[43] C. Weisbuch and C. Hermann, Optical detection of conduction-electron spin resonance in GaAs, $Ga_{1-x}In_xAs$, and $Ga_{1-x}Al_xAs$, Phys. Rev. B **15**, 816 (1977).

[44] M. Dobers, J. P. Vieren, Y. Guldner, P. Bove, F. Omnes, and M. Razeghi, Electron-spin resonance of the two-dimensional electron gas in $Ga_{0.47}In_{0.53}As$-InP heterostructures, Phys. Rev. B **40**, R8075 (1989).

[45] B. Kowalski, P. Omling, B. K. Meyer, D. M. Hofmann, V. Härle, F. Scholz, and P. Sobkowicz, Optically detected spin resonance of conduction band electrons in InGaAs/InP quantum wells, Semicond. Sci. Technol. **11**, 1416 (1996).

[46] J. Zhou, J. L. Cheng, and M. W. Wu, Spin relaxation in *n*-type GaAs quantum wells from a fully microscopic approach, Phys. Rev. B **75**, 045305 (2007).

[47] Y. Egami and H. Akera, Controlling Rashba spin-orbit interaction in quantum wells by adding symmetric potential, Appl. Phys. Express **10**, 063007 (2017).

[48] F. Capasso, A. Y. Cho, K. Mohammed, and P. W. Foy, Doping interface dipoles: Tunable heterojunction barrier heights and band-edge discontinuities by molecular beam epitaxy, Appl. Phys. Lett. **46**, 664 (1985).

[49] S. Modesti, D. Furlanetto, M. Piccin, S. Rubini, and A. Franciosi, High-resolution potential mapping in semiconductor nanostructures by cross-sectional scanning tunneling microscopy and spectroscopy, Appl. Phys. Lett. **82**, 1932 (2003).

[50] M. Q. Weng and M. W. Wu, Multisubband effect in spin dephasing in semiconductor quantum wells, Phys. Rev. B **70**, 195318 (2004).

[51] T. Kaneko, M. Koshino, and T. Ando, Numerical study of spin relaxation in a quantum wire with spin-orbit interaction, Phys. Rev. B **78**, 245303 (2008).